An Advanced Meshless Method for Time Fractional Diffusion Equation

Y. T. Gu

[1]School of Engineering Systems, Queensland University of Technology, Australia
G. P. O. Box 2434, Brisbane, QLD 4001, Australia
(e-mail of corresponding author: yuantong.gu@qut.edu.au)

P. Zhuang, Q. Liu

[2]School of Mathematical Sciences,

Xiamen University, China.

Abstract

Recently, because of the new developments in sustainable engineering and renewable energy, which are usually governed by a series of fractional partial differential equations (FPDEs), the numerical modelling and simulation for fractional calculus are attracting more and more attention from researchers. The current dominant numerical method for modeling FPDE is Finite Difference Method (FDM), which is based on a pre-defined grid leading to inherited issues or shortcomings including difficulty in simulation of problems with the complex problem domain and in using irregularly distributed nodes. Because of its distinguished advantages, the meshless method has good potential in simulation of FPDEs. This paper aims to develop an implicit meshless collocation technique for FPDE. The discrete system of FPDEs is obtained by using the meshless shape functions and the meshless collocation formulation. The stability and convergence of this meshless approach are investigated theoretically and numerically. The numerical examples with regular and irregular nodal distributions are used to validate and investigate accuracy and efficiency of the newly developed meshless formulation. It is concluded that the present meshless formulation is very effective for the modeling and simulation of fractional partial differential equations.

Key words: Fractional differential equation, Meshless method, Moving least squares, RBF, Collocation formulation.

1. Introduction

Many problems in engineering and science are governed by a serial of differential equations with an integer differential order. Recently, it has noted that many problems in modern engineering such as in sustainable environment and renewable energy are better to be described by fractional calculus than the normal integral calculus. In these problems, the governing equations are so-called fractional ordinary differential equations (FODE) or fractional partial differential equations (FPDE) (Agrawal et al., 2004; Benson et al., 2000; Butzer and Georges, 2000). For example, it has been reported that, in numerous physical and biological systems, many diffusion rates of species cannot be characterized by the single parameter of the diffusion constant (Sokolov and Klafter, 2005). Instead, the anomalous diffusion is characterized by a scaling fractional parameter α as well as a diffusion constant κ.

The modeling of FODEs or FPDEs has become a new hot topic in computational mechanics and computational mathematics (Liu et al., 2011; Zhuang el al., 2008). Unlike the normal PDE, the differential order (regarding to time or space or both) in a FPDE is not with a integer order, in other words, with a fractional order (i.e., 0.5th order, 1.5th order, and so on), which will lead to a big difficulty and new challenge in numerical simulation, because existing numerical simulation techniques are developed for PDE with integer differential orders. At present, most of FPDEs are solved numerically by Finite Difference Method (FDM) (Liu and Zhuang et al., 2007; Meerschaert and Tadjeran, 2004), when a few of research has been reported using Finite Element Method (FEM)(Ervin and Roop, 2004, 2007). FDM and FEM are numerical approaches based on pre-defined meshes/grids, which lead to inherited issues or shortcomings including: difficulty in handling a complex problem domain and irregular nodal distribution; difficulty in conducting adaptive analysis, and low computational accuracy. Therefore, these shortcomings become a main barrier for the development of a powerful numerical simulation tool for practical engineering/science applications governed by FPDEs. This is also the major reason why most current research in this field are still limited in some one-dimensional (1-D) or two-dimensional (2-D) benchmark problems with very simple problem domains (i.e., squares and rectangles) and Dirichlet boundary conditions.

In past 20 years, much effort has been directed toward the development of meshless methods in computational mechanics(Liu and Gu, 2005). There are many categories of meshless method (Gu, 2005), and group of meshless methods have been developed including the meshless collocation methods (Kensa, 1990; Onate et al., 1996), the smooth particle hydrodynamics (SPH)(Gingold and Moraghan,1977), the element-free Galerkin (EFG) method (Belytschko et al., 1994), the reproducing kernel particle method (RKPM) (Liu and Jun et al., 1995), and the point interpolation method (PIM) (Liu and Gu, 2001b). To alleviate the global integration background cells (Liu and Gu, 2002), the meshless methods based on the local weak-forms and the boundary integral equation (BIE) have also been developed, for example, the meshless local Petrov-Galerkin (MLPG) method (Atluri and Zhu, 1998), the local radial point interpolation method (LRPIM)(Gu et al. 2007; Liu and Gu, 2001a), the boundary node method (BNM) (Mukherjee and Mukherjee,1997), and the boundary point interpolation method (BPIM)(Gu and Liu, 2002, 2003). These meshless methods have found many applications in engineering and science (Gu and Liu, 2003; Liu and Gu, 2005).

In spite of the impressive progresses, there are still some technical issues (Liu and Gu, 2004) in the development of meshless techniques, for instance, a) the lack of theoretical study on the computational convergence and stability; b) the relatively lower computational efficiency; and c) the lack of commercial software packages for meshless analyses. Recently, some deep researches have been conducted and the above issues have been partially resolved. Liu et al. Liu and Zhang, 2008) proposed a node-based smoothed point interpolation method (NS-PIM), which is formulated using the polynomial point interpolation method (PIM)(Liu and Gu, 2001b) or the radial point interpolation method (RPIM))Liu and Gu, 2001a). It was found that NS-PIM behaves 'overly-soft', leading to the so-called temporal instability when used to solve dynamic problems. The formulation was also elaborated with a theoretical base on the G space theory (Liu, 2009). Invoking the G space theory and the weakened weak-form (W2)(Liu, 2008), the meshless (or smoothed FEM) methods show a number of attractive properties, e.g., conformability, softness, upper/lower bound, super-convergence, ultra accuracy, and they also work well with triangular background cells .

Comparing with traditional FDM and FEM, the meshless methods have demonstrated some distinguished advantages (Liu and Gu, 2005) including: a) They do not use a mesh, so that the burden of mesh generation in FDM and FEM is overcome. Hence, an adaptive analysis is easily achievable; b)They are usually more accurate than FDM due to the use of higher order meshless trial functions; c) They are capable of solving complex problems that are difficult for the conventional FDM and FEM. Because of these unique advantages, the meshless method should have a good potential for the simulation of FPDEs. However, to the authors' best knowledge, very limited work was reported to handle fractional partial differential equations (FPDE) by the meshless techniques (Chen, Ye et al., 2010; Gu, Zhuang and Liu, 2010).Therefore, this topic calls for a significant development.

The objective of this paper is to develop an implicit meshless formulation based on the meshless shape functions and the meshless collocation formulation for numerical simulation of fractional partial differential equations (FPDEs). We will mostly focus on the time fractional diffusion equation (TFDE), which is a typical FPDE. The discrete equations for two-dimensional TFDEs are obtained by using the meshless shape functions and the strong-forms. The stability and convergence of this method are then discussed and investigated. Numerical examples with different nodal distributions are used to validate and investigate accuracy and efficiency of the newly developed meshless formulation. Some key parameters, which affect the performance of this meshless technique, are thoroughly investigated and the optimized parameters are recommended.

2. Moving least squares shape functions

Several meshless approximation formulations have been proposed[32]. The moving least squares (MLS) approximation is one of the widely used meshless methods because of its' attractive properties of accuracy, robustness, and higher-order of continuity.

Consider an unknown scalar function of a field variable $u(\mathbf{x})$ in the domain, Ω. The MLS approximation of $u(\mathbf{x})$ is defined at $\mathbf{x}$ as (Liu and Gu, 2005)

$$u^h(\mathbf{x}) = \sum_{j=1}^{m} p_j(\mathbf{x}) a_j(\mathbf{x}) = \mathbf{p}^{\mathrm{T}}(\mathbf{x})\mathbf{a}(\mathbf{x}) \tag{1}$$

where $\mathbf{p}(\mathbf{x})$ is the basis function of the spatial coordinates, $\mathbf{x}^{\mathrm{T}}=[x, y]$ for two-dimensional problem, and m is the number of the basis functions.

In Equation (1), $\mathbf{a}(\mathbf{x})$ is a vector of coefficients, which is a function of $\mathbf{x}$. The coefficients $\mathbf{a}$ can be obtained by minimizing the following weighted discrete $\mathbf{L}_2$ norm.

$$J = \sum_{i=1}^{n} \widehat{W}(\mathbf{x}-\mathbf{x}_i)[\mathbf{p}^{\mathrm{T}}(\mathbf{x}_i)\mathbf{a}(\mathbf{x}) - u_i]^2 \tag{2}$$

where n is the number of nodes in the support domain of $\mathbf{x}$ for which the weight function $\widehat{W}(\mathbf{x}-\mathbf{x}_i) \neq 0$. Because the number of nodes, n, used in the MLS approximation is usually much larger than the number of unknown coefficients, m, the approximated function, u^h, does not pass through the nodal values.

The stationarity of J with respect to $\mathbf{a}(\mathbf{x})$ gives $\partial J / \partial \mathbf{a} = 0$ which leads to the following set of linear relations.

$$\mathbf{A}(\mathbf{x})\mathbf{a}(\mathbf{x})=\mathbf{B}(\mathbf{x})\mathbf{U}_s \tag{3}$$

where $\mathbf{U}_s$ is the vector that collects the nodal parameters of field function for all the nodes in the support domain. **A**(**x**) is called the weighted moment matrix defined by

$$\mathbf{A}(\mathbf{x}) = \sum_{i=1}^{n} \widehat{W}_i(\mathbf{x})\mathbf{p}(\mathbf{x}_i)\mathbf{p}^{\mathrm{T}}(\mathbf{x}_i) \tag{4}$$

The matrix **B** in Equation (24) is defined as

$$\mathbf{B}(\mathbf{x})=[\widehat{W}_1(\mathbf{x})\mathbf{p}(\mathbf{x}_1) \;\; \widehat{W}_2(\mathbf{x})\mathbf{p}(\mathbf{x}_2) \ldots \;\; \widehat{W}_n(\mathbf{x})\mathbf{p}(\mathbf{x}_n)] \tag{5}$$

Solving Equation (24) for **a**(**x**), we have

$$\mathbf{a}(\mathbf{x}) = \mathbf{A}^{-1}(\mathbf{x})\mathbf{B}(\mathbf{x})\mathbf{U}_s \tag{6}$$

Substituting the above equation back into Equation (1), we obtain

$$u^h(\mathbf{x}) = \sum_{i=1}^{n} \phi_i(\mathbf{x})u_i = \mathbf{\Phi}^{\mathrm{T}}(\mathbf{x})\mathbf{U}_s \tag{7}$$

where $\mathbf{\Phi}(\mathbf{x})$ is the vector of MLS shape functions corresponding n nodes in the support domain of the point **x**, and can be written as,

$$\mathbf{\Phi}^{\mathrm{T}}(\mathbf{x}) = \{\phi_1(\mathbf{x}) \quad \phi_2(\mathbf{x}) \quad \cdots \quad \phi_n(\mathbf{x})\} = \mathbf{p}^{\mathrm{T}}(\mathbf{x})\mathbf{A}^{-1}(\mathbf{x})\mathbf{B}(\mathbf{x}) \tag{8}$$

For the convenience in obtaining the partial derivatives of the shape functions, Equation (8) is re-written as (Liu and Gu, 2005)

$$\mathbf{\Phi}^{\mathrm{T}}(\mathbf{x}) = \boldsymbol{\gamma}^{\mathrm{T}}(\mathbf{x})\mathbf{B}(\mathbf{x}) \tag{9}$$

where

$$\boldsymbol{\gamma}^{\mathrm{T}} = \mathbf{p}^{\mathrm{T}}\mathbf{A}^{-1}, \quad \text{then} \quad \mathbf{A}\boldsymbol{\gamma} = \mathbf{p} \tag{10}$$

The partial derivatives of $\boldsymbol{\gamma}$ can then be obtained by solving the following equations.

$$\begin{aligned} &\mathbf{A}\boldsymbol{\gamma}_{,i} = \mathbf{p}_{,i} - \mathbf{A}_{,i}\boldsymbol{\gamma}, \quad \mathbf{A}\boldsymbol{\gamma}_{,ij} = \mathbf{p}_{,ij} - (\mathbf{A}_{,i}\boldsymbol{\gamma}_{,j} + \mathbf{A}_{,j}\boldsymbol{\gamma}_{,i} + \mathbf{A}_{,ij}\boldsymbol{\gamma}) \\ &\mathbf{A}\boldsymbol{\gamma}_{,ijk} = \mathbf{p}_{,ijk} - (\mathbf{A}_{,i}\boldsymbol{\gamma}_{,jk} + \mathbf{A}_{,j}\boldsymbol{\gamma}_{,ik} + \mathbf{A}_{,k}\boldsymbol{\gamma}_{,ij} + \mathbf{A}_{,ij}\boldsymbol{\gamma}_{,k} \\ &\qquad + \mathbf{A}_{,ik}\boldsymbol{\gamma}_{,j} + \mathbf{A}_{,jk}\boldsymbol{\gamma}_{,i} + \mathbf{A}_{,ijk}\boldsymbol{\gamma}) \end{aligned} \tag{11}$$

where i, j and k denote coordinates x and y, and a comma designates a partial derivative with respect to the indicated spatial coordinate that follows. The partial derivatives of the shape function $\mathbf{\Phi}$ can be obtained using the following expressions.

$$\begin{aligned} &\mathbf{\Phi}^{\mathrm{T}}_{,i} = \boldsymbol{\gamma}^{\mathrm{T}}_{,i}\mathbf{B} + \boldsymbol{\gamma}^{\mathrm{T}}\mathbf{B}_{,i}, \quad \mathbf{\Phi}^{\mathrm{T}}_{,ij} = \boldsymbol{\gamma}^{\mathrm{T}}_{,ij}\mathbf{B} + \boldsymbol{\gamma}^{\mathrm{T}}_{,i}\mathbf{B}_{,j} + \boldsymbol{\gamma}^{\mathrm{T}}_{,j}\mathbf{B}_{,i} + \boldsymbol{\gamma}^{\mathrm{T}}\mathbf{B}_{,ij} \\ &\mathbf{\Phi}^{\mathrm{T}}_{,ijk} = \boldsymbol{\gamma}^{\mathrm{T}}_{,ijk}\mathbf{B} + \boldsymbol{\gamma}^{\mathrm{T}}_{,ij}\mathbf{B}_{,k} + \boldsymbol{\gamma}^{\mathrm{T}}_{,ik}\mathbf{B}_{,j} + \boldsymbol{\gamma}^{\mathrm{T}}_{,jk}\mathbf{B}_{,i} \\ &\qquad + \boldsymbol{\gamma}^{\mathrm{T}}_{,i}\mathbf{B}_{,jk} + \boldsymbol{\gamma}^{\mathrm{T}}_{,j}\mathbf{B}_{,ik} + \boldsymbol{\gamma}^{\mathrm{T}}_{,k}\mathbf{B}_{,ij} + \boldsymbol{\gamma}^{\mathrm{T}}\mathbf{B}_{,ijk} \end{aligned} \tag{12}$$

Equation (8) shows that the continuity of the MLS shape function $\mathbf{\Phi}$ is governed by the continuity of the basis function $\mathbf{p}$ as well as the smoothness of the matrices $\mathbf{A}$ and $\mathbf{B}$. The latter is governed by the smoothness of the weight function. Therefore, the weight function plays an important role in the performance of the MLS approximation.

The exponential function and spline functions are often used in practice. Among them, the most commonly used quartic spline weight function is given by (Liu and Gu, 2005)

$$\widehat{W}_i(\mathbf{x}) = \begin{cases} 1-6\bar{r}_i^2+8\bar{r}_i^3-3\bar{r}_i^4 & \bar{r}_i \le 1 \\ 0 & \bar{r}_i > 1 \end{cases} \tag{13}$$

3 Time fractional diffusion equation

The time fractional diffusion equation can be written in the following form

$$\frac{\partial^\alpha u(\mathbf{x},t)}{\partial t^\alpha} = \kappa \Delta u(\mathbf{x},t) + f(\mathbf{x},t),\ \ \mathbf{x} \in \Omega \subset \mathbf{R}^2,\ \ t>0 \tag{14}$$

together with the general boundary and initial conditions

$$u(\mathbf{x},t) = g(\mathbf{x},t),\ \ \mathbf{x} \in \partial\Omega,\ \ t>0 \tag{15}$$

$$u(\mathbf{x},0) = u_0(\mathbf{x}),\ \ \mathbf{x} \in \Omega \tag{16}$$

where Δ is the Laplace differential operator, Ω a bounded domain in $\mathbf{R}^2$, $\partial\Omega$ the boundary of Ω, κ the diffusion coefficient, $f(\mathbf{x},t)$, $g(\mathbf{x},t)$ and $u_0(\mathbf{x})$ are known functions.

In Equation (14), $\frac{\partial^\alpha u(\mathbf{x},t)}{\partial t^\alpha}$ is the Caputo fractional derivative of order $\alpha\,(0<\alpha<1)$ defined as

$$\frac{\partial^\alpha u(\mathbf{x},t)}{\partial t^\alpha} = \frac{1}{\Gamma(1-\alpha)}\int_0^t (t-\eta)^{-\alpha}\frac{\partial u(\mathbf{x},\eta)}{\partial \eta}\mathrm{d}\eta \tag{17}$$

2.1 Time discretization

Define $t_k = k\Delta t$, $k=1,2,\cdots,n$, where Δt is time step size. The time fractional derivative at $t=t_{k+1}$ can be approximated by

$$\frac{\partial^\alpha u(\mathbf{x},t_{k+1})}{\partial t^\alpha} = \frac{1}{\Gamma(1-\alpha)}\sum_{j=0}^{k}\int_{t_j}^{t_{j+1}} (t_{k+1}-\eta)^{-\alpha}\frac{\partial u(\mathbf{x},\eta)}{\partial \eta}\mathrm{d}\eta \tag{18}$$

$$=\frac{1}{\Gamma(1-\alpha)}\sum_{j=0}^{k}\frac{u\left(\mathbf{x},t_{j+1}\right)-u\left(\mathbf{x},t_{j}\right)}{\Delta t}\int_{t_j}^{t_{j+1}}\left(t_{k+1}-\eta\right)^{-\alpha}\mathrm{d}\eta+\tilde{R}_{k+1}$$

where the truncation error R_{k+1} satisfies

$$\left|\tilde{R}_{k+1}\right|\le C\left(\Delta t\right)^{2-\alpha} \tag{19}$$

Let $b_j=\left(j+1\right)^{1-\alpha}-j^{1-\alpha}$, $j=0,1,2,\cdots,n$, then Equation (18) can be rewritten as

$$\frac{\partial^{\alpha}u\left(\mathbf{x},t_{k+1}\right)}{\partial t^{\alpha}}=\frac{\left(\Delta t\right)^{-\alpha}}{\Gamma\left(2-\alpha\right)}\sum_{j=0}^{k}b_{k-j}\left[u\left(\mathbf{x},t_{j+1}\right)-u\left(\mathbf{x},t_{j}\right)\right]+\tilde{R}_{k+1} \tag{20}$$

or

$$\frac{\partial^{\alpha}u\left(\mathbf{x},t_{k+1}\right)}{\partial t^{\alpha}}=\frac{\left(\Delta t\right)^{-\alpha}}{\Gamma\left(2-\alpha\right)}\sum_{j=0}^{k}b_{j}\left[u\left(\mathbf{x},t_{k-j+1}\right)-u\left(\mathbf{x},t_{k-j}\right)\right]+\tilde{R}_{k+1} \tag{21}$$

Substituting Equation (21) into Equation (18), we obtain

$$\begin{aligned}&u\left(\mathbf{x},t_{k+1}\right)-\mu_1\Delta u\left(\mathbf{x},t_{k+1}\right)\\&\quad=u\left(\mathbf{x},t_{k}\right)-\sum_{j=1}^{k}b_{j}\left[u\left(\mathbf{x},t_{k-j+1}\right)-u\left(\mathbf{x},t_{k-j}\right)\right]+\mu_2 f\left(\mathbf{x},t_{k+1}\right)+R_{k+1}\end{aligned} \tag{22}$$

where $\mu_1=\kappa\left(\Delta t\right)^{\alpha}\Gamma\left(2-\alpha\right)$, $\mu_2=\left(\Delta t\right)^{\alpha}\Gamma\left(2-\alpha\right)$ and

$$\left|R_{k+1}\right|\le\tilde{C}\left(\Delta t\right)^{2} \tag{23}$$

where $\tilde{C}$ is a positive constant.

Let $u^k=u^k\left(\mathbf{x}\right)$ be the numerical approximation to $u\left(\mathbf{x},t_k\right)$ and $F^{k+1}=\mu_2 f\left(\mathbf{x},t_{k+1}\right)$, then Equations (18) - (20) can be discretized as the following scheme

$$u^{k+1}-\mu_1\Delta u^{k+1}=u^{k}-\sum_{j=1}^{k}b_{j}\left[u^{k+1-j}-u^{k-j}\right]+F^{k+1},\ k=0,1,\cdots,n-1 \tag{24}$$

$$u^{0}=u_{0}\left(\mathbf{x}\right) \tag{25}$$

$$u^{k}\Big|_{\partial\Omega}=g\left(\mathbf{x},t_{k}\right),\ k=0,1,\cdots,n \tag{26}$$

2.2 Spatial discretization

Consider the following fractional partial differential equation as presented in Equation (24)

$$u^{k+1}-\mu_1\Delta u^{k+1}=u^{k}-\sum_{j=1}^{k}b_{j}\left[u^{k+1-j}-u^{k-j}\right]+F^{k+1},\ \text{ in }\Omega \tag{27}$$

together with Dirichlet boundary condition

$$u^{k+1}(\mathbf{x}) = g(\mathbf{x}, t_{k+1}), \text{ on } \partial\Omega \tag{28}$$

Assume that there are N_d internal (domain) points and N_b boundary points. Hence, the following N_d equations at internal domain nodes can be obtained

$$\hat{u}^{k+1} - \mu_1 \Delta \hat{u}^{k+1} = \hat{u}^k - \sum_{j=1}^{k} b_j \left[\hat{u}^{k+1-j} - \hat{u}^{k-j} \right] + F^{k+1}, \text{ in } \Omega \tag{29}$$

The following N_b equations are satisfied on $\partial\Omega$

$$\hat{u}_i^{k+1} = g\left(\mathbf{x}_i, t_{k+1}\right), \; i = 1, 2, \cdots, N_b \,. \tag{30}$$

Thus based on MLS shape function, Equation (7), we have

$$\hat{u}^{k+1}\left(\mathbf{x}\right) = \sum_{i=1}^{n} \Phi_i \hat{u}_i^{k+1} \tag{31}$$

and its derivatives can be obtained by the following equations

$$\frac{\partial^l \hat{u}^{k+1}\left(\mathbf{x}\right)}{\partial x^l} = \sum_{i=1}^{n} \frac{\partial^l \Phi_i}{\partial x^l} \hat{u}_i^{k+1} \tag{32}$$

$$\frac{\partial^l \hat{u}^{k+1}\left(\mathbf{x}\right)}{\partial y^l} = \sum_{i=1}^{n} \frac{\partial^l \Phi_i}{\partial y^l} \hat{u}_i^{k+1} \tag{33}$$

Thus, $\hat{u}_i^{k+1}$ and its derivatives in Equation (29) can be obtained by substituting $\mathbf{x}$ into $\mathbf{x}_i$ in Equations (32) ~ (33)

$$\hat{u}_i^{k+1} = \hat{u}^{k+1}\left(\mathbf{x}_i\right), \; \frac{\partial^2 \hat{u}_i^{k+1}}{\partial x^2} = \frac{\partial^2 \hat{u}^{k+1}\left(\mathbf{x}_i\right)}{\partial x^2}, \; \frac{\partial^2 \hat{u}_i^{k+1}}{\partial y^2} = \frac{\partial^2 \hat{u}^{k+1}\left(\mathbf{x}_i\right)}{\partial y^2} \tag{34}$$

4 Numerical examples

In this section, some numerical examples are studied to demonstrate the effectiveness of the newly proposed meshless approach. We solve the following time fractional advection-diffusion equation

$$\frac{\partial^\alpha u\left(\mathbf{x}, t\right)}{\partial t^\alpha} = \kappa \Delta u\left(\mathbf{x}, t\right) + f\left(\mathbf{x}, t\right), \; \mathbf{x} \in \Omega \subset \mathbf{R}^2, \; t > 0 \tag{35}$$

$$u\left(\mathbf{x}, t\right) = t^2 e^{x+y}, \; \mathbf{x} \in \partial\Omega, \; t > 0 \tag{36}$$

$$u\left(\mathbf{x}, 0\right) = 0, \; \mathbf{x} \in \Omega \tag{37}$$

where we employ $\kappa = 1.0$, and

$$f\left(\mathbf{x}, t\right) = \left[\frac{2t^{2-\alpha}}{\Gamma\left(3-\alpha\right)} - 2t^2 \right] e^{x+y} \tag{38}$$

The exact solution of Equations (35)-(37) is (Gu, Zhuang et al., 2010)

$$u(\mathbf{x},t) = t^2 e^{x+y} \tag{39}$$

As a fraction order in Equation (35), we take

$$\alpha = 0.85 \tag{40}$$

For quantitative studies, the following error notations are introduced

$$\varepsilon_{\max} = \max_i \left| u_i^{exact} - u_i^{num} \right|, \qquad \varepsilon_0 = \sqrt{\frac{\sum_{i=1}^{N} (u_i^{exact} - u_i^{num})^2}{\sum_{i=1}^{N} (u_i^{exact})^2}}, \tag{41}$$

$$\varepsilon_x = \sqrt{\frac{\sum_{i=1}^{N} (u_{i,x}^{exact} - u_{i,x}^{num})^2}{\sum_{i=1}^{N} (u_{i,x}^{exact})^2}}, \qquad \varepsilon_y = \sqrt{\frac{\sum_{i=1}^{N} (u_{i,y}^{exact} - u_{i,y}^{num})^2}{\sum_{i=1}^{N} (u_{i,y}^{exact})^2}} \tag{42}$$

where N denotes the number of nodes; u_i^{exact} and u_i^{num} are exact and numerical solutions, respectively, for interest point *i*; and $u_{i,}$ denotes the derivative.

The $L-$shaped problem domain, given by the following equation and plotted in Fig. 1, is considered

$$\Omega = \left\{ (x, y) \middle| 0 \le x, y \le 1, sign(x-0.5) + sign(y-0.5) \le 0 \right\} \tag{43}$$

The regularly distributed nodes, as shown in Fig. 1, are firstly used to discretize this L-shaped problem domain. The computational errors for different time steps are plotted in Fig. 2 and listed in Table 1, which have proven that the proposed meshless approach performs very well for this case in terms of accuracy and convergence. The convergent rate is in the order of $O(\Delta t^{2-\alpha})$. For comparison, the conventional FDM is also used to simulate this problem. It has found that if the same regular nodal distributions are used, the present meshless approach leads to more accurate results than FDM.

Table 1: The computational error obtained using meshless approach at *t* = 1.0 (Regular nodal distribution on *L*-shaped region)

Δt	$\varepsilon_{\max}$	$R_{\varepsilon\max}$	ε_0	$R_{\varepsilon 0}$	ε_x	$R_{\varepsilon x}$	ε_y	$R_{\varepsilon y}$
0.1	4.351e-3	---	1.022e-3	---	4.856e-3	---	4.856e-3	---
0.05	1.967e-3	2.212	4.619e-4	2.213	2.195e-3	2.212	2.195e-3	2.212
0.025	8.888e-4	2.213	2.088e-4	2.212	9.919e-4	2.213	9.919e-4	2.213
0.0125	4.024e-4	2.209	9.451e-5	2.209	4.489e-4	2.210	4.489e-4	2.210

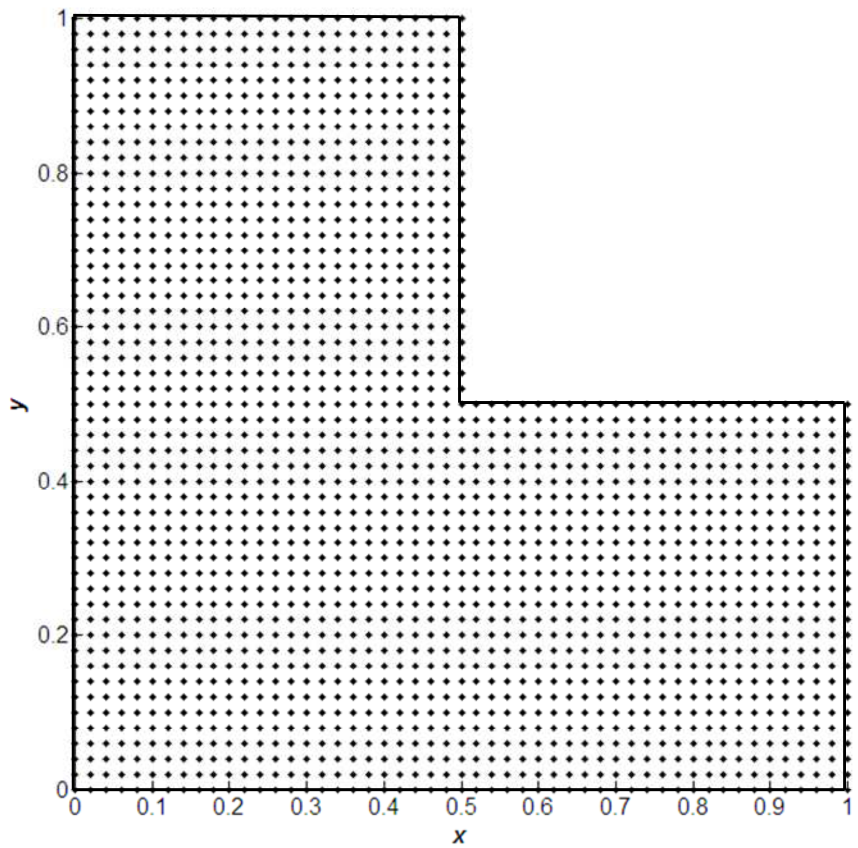

Figure 1: 1976 Regular distribution of points on *L*-shaped domain

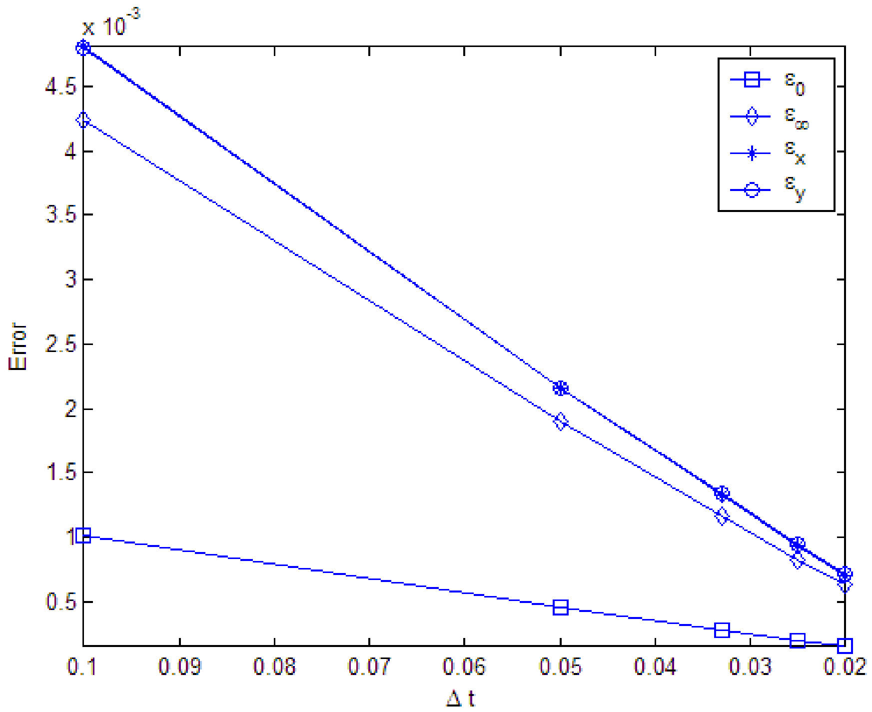

Figure 2: Errors as a function of the time step Δt (Regular nodal distribution on *L*-shaped region)

The irregularly distributed nodes are also used for this problem with an *L*-shaped region, as shown in Fig. 3. The computational errors for different time steps are plotted in Fig. 4 and listed in Table 2. It can be concluded that the present meshless approach also leads to good computational accuracy and convergent rates for this *L*-shaped case using irregularly distributed nodes. It has proven the effectiveness of the meshless approach for a problem with a complex problem domain and irregular nodal distribution.

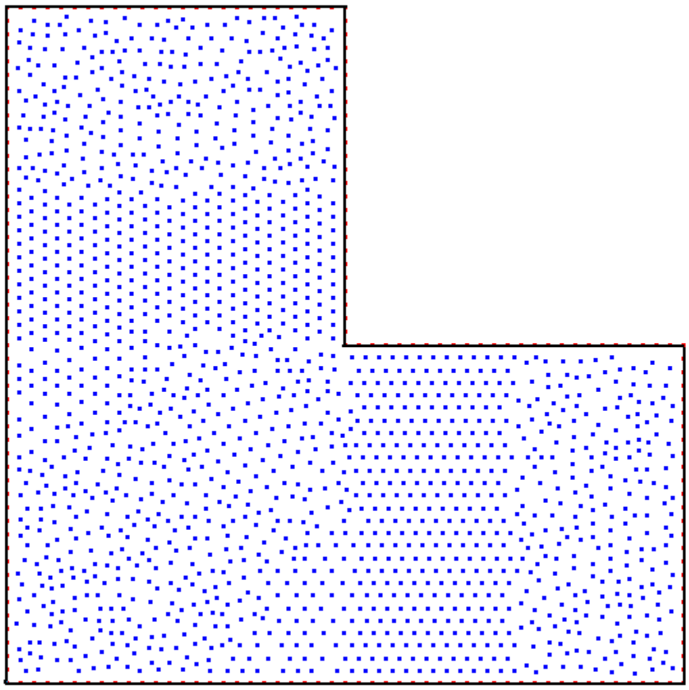

Figure 3: Irregular distribution of points on *L*-shaped domain

Table 2: The error obtained using meshless approach at $t = 1.0$ (Irregular nodal distribution on $L-$shaped region)

Δt	$\varepsilon_{\max}$	$R_{\varepsilon\max}$	ε_0	$R_{\varepsilon 0}$	ε_x	$R_{\varepsilon x}$	ε_y	$R_{\varepsilon y}$
0.1	4.242e-3	---	1.010e-3	---	4.805e-3	---	4.792e-3	---
0.05	1.900e-3	2.233	4.544e-4	2.223	2.152e-3	2.233	2.157e-3	2.222
0.025	8.266e-4	2.299	1.992e-4	2.281	9.354e-4	2.301	9.460e-4	2.280
0.0125	3.606e-4	2.292	8.412e-5	2.368	3.887e-4	2.406	4.019e-4	2.353

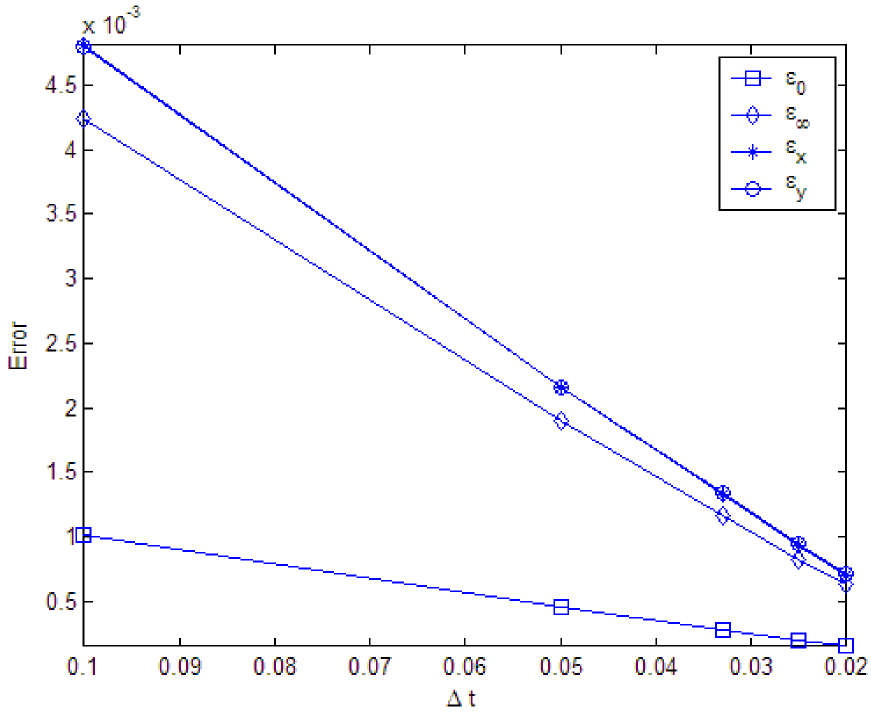

Figure 4: Errors as a function of the time step Δt (Irregular nodal distribution on *L*-shaped region)

6. Conclusion

This paper has proposed an implicit meshless approach based on the moving least squares (MLS) and the meshless collocation formulation for numerical simulation of fractional partial differential equations (FPDE). The discrete system of equations is firstly obtained, and the numerical example is then used to validate and investigate accuracy and efficiency of the newly developed meshless formulation. It has been found that the present implicit meshless formulation for FPDEs is un-conditionally stable. If the same regular nodal distributions are used, the present meshless approach leads to more accurate results than FDM. The present meshless approach has good accuracy and convergence for irregular nodal distributions and complex problem domains.

In summary, the newly developed meshless approach is accurate and convergent. Most importantly, the present approach is robust for arbitrarily distributed nodes and complex problem domains, for which the conventional FDM is difficult to handle. Hence, the present meshless formulation is very effective for the modeling and simulation of fractional differential equations.

References

Agrawal O. P., Machado J. A. T. and Sabatier J. (2004), Introduction. Nonlinear Dynam. 38:1-2.

Atluri S.N. and Zhu T. (1998), A new meshfree local Petrov-Galerkin (MLPG) approach in computational mechanics. Computational Mechanics, 22: 117-127.

Belytschko T, Lu Y.Y. and Gu L. (1994): Element-free Galerkin methods. Int. J. Numer. Methods Engrg., vol. 37, pp. 229–256.

Benson D.A., Wheatcraft S. W., and Meerschaert M. M.(2000), Application of a fractional advection-dispertion equation. Water Resour. Res. 36(6): 1403-1412.

Butzer P. L. and Georges A.(2000), An Introduction to Fractional Calculus. World Scientific. Singapore.

Chen W., Ye L. and Sun H. (2010): Fractional diffusion equations by the Kansa method. Computers and Mathematics with Applications. vol. 59(5), pp. 1614–1620.

Ervin V. J. and Roop J. P., Variational formulation for the stationary fractional advection dispersion equation. Numerical Methods Partial Differential Equations 2004; 22: 558-576.

Ervin V. J., Heuer N. and Roop J. P., Numerical approximation of a time dependent, nonlinear, space-fractional diffusion equation. SIAM Journal of Numerical Analysis 2007; 45: 572-591.

Gingold R.A. and Moraghan J.J. (1977), Smooth particle hydrodynamics: theory and applications to non spherical stars. Monthly Notices of the Royal Astronomical Society, 181, 375-389.

Gu Y.T. (2005), Meshfree methods and their comparisons. International Journal of Computational Methods. 2(4), 477-515.

Gu Y.T. and Liu G.R. (2002), A boundary point interpolation method for stress analysis of solids. Computational Mechanics, 28, 47-54.

Gu Y.T. and Liu G.R. (2003), A boundary radial point interpolation method (BRPIM) for 2-D structural analyses. Structural Engineering and Mechanics, 15 (5), 535-550.

Gu Y.T., Wang Q.X., and Lam K.Y.(2007), A meshless local Kriging method for large deformation analyses. Computer Methods in Applied Mechanics and Engineering. 196(9-12), 1673-1684.

Gu Y.T. and Liu G.R.(2003), Hybrid boundary point interpolation methods and their coupling with the element free Galerkin method. Engineering Analysis with Boundary Element, 27(9), 905-917.

Gu Y.T., Zhuang P. and Liu F.(2010), An Advanced Implicit Meshless Approach for the Non-linear Anomalous Subdiffusion Equation. CMES, vol.56, no.3, pp.303-333.

Kansa E. J. (1990): Multiquadrics-A Scattered Data Approximation Scheme with

Applications to Computational Fluid dynamics. Computers Math. Applic., vol. 19(8/9), pp. 127–145.

Liu F., Zhuang P., Anh V., Turner I. and Burrage K.(2007), Stability and convergence of the difference methods for the space-time fractional advection-diffusion equation, Applied Mathematics and Computation, 191: 12–20.

Liu G.R. and Gu Y.T. (2001a), A local radial point interpolation method (LR-PIM) for free vibration analyses of 2-D solids. Journal of Sound and Vibration, 246(1): 29-46.

Liu G.R. and Gu Y.T.(2001b), A point interpolation method for two-dimensional solids. International Journal for Numerical Methods in Engineering, 50 (4), 937-951.

Liu G.R. and Gu Y. T. (2005), An introduction to meshfree methods and their programming. Springer Press, Berlin.

Liu G.R. and Gu Y.T.(2002), Comparisons of two meshfree local point interpolation methods for structural analyses. Computational Mechanics, 29(2), 107-121.

Liu G.R., Gu Y.T. and Dai K.Y. (2004), Assessment and applications of point interpolation methods for computational mechanics. Int. J. for Numerical Methods in Eng. 59(10): 1373-1397.

Liu G. R. and Zhang G. Y., Upper bound solution to elasticity problems: A unique property of the linearly conforming point interpolation method (LC-PIM). International Journal for Numerical Methods in Engineering, 74 (2008), 1128–1161

Liu G. R., On G space theory. International Journal of Computational Methods. 6(2) (2009), 257–289

Liu G. R., A G space and weakened weak (W2) form for a unified formulation of compatible and incompatible methods, part I–Theory and part II–Application to solid mechanics problems, International Journal for Numerical Methods in Engineering, 2008

Liu Q.X., Gu Y.T，Zhuang P., Liu F. and Nie Y.F. (2011), An implicit RBF meshless approach for time fractional diffusion equations. Computational Mechanics (in press).

Liu W.K., Jun S. and Zhang Y. (1995), Reproducing kernel particle methods. International Journal for Numerical Methods in Engineering, 20: 1081-1106.

Meerschaert M. and Tadjeran C.(2004), Finite difference approximations for fractional advection-dispersion flow equations. J. comput. Appl. Math., 172: 65–77.

Mukherjee Y.X. and Mukherjee S. (1997), Boundary node method for potential problems. Int. J. Num. Methods in Engrg. 40, 797-815.

Onate E., Idelsohn S., Zienkiewicz O. C., Taylor R. L. and Sacco C. (1996): A finite method in computational mechanics: applications to convective transport and fluid flow. International Journal of Numerical Methods in Engineering, vol. 39, pp. 3839–3866.

Sokolov I. and Klafter J. (2005), From diffusion to anomalous diffusion: a century after Einstein's brownian motion. Chaos, vol. 15, 026103.

Zhuang P., Liu, F., Anh V. and Turner I. (2008): New solution and analytical techniques of the implicit numerical method for the anomalous subdiffusion equation. SIAM Journal on Numerical Analysis, vol. 46(2), pp. 1079–1095.